Study of Shower Optical Image Based on Energy Deposits Derived from CORSIKA

D. Góra[1], D. Heck[2], P. Homola[1], H. Klages[2], J. Pękala[1], M. Risse[2], B. Wilczyńska[1] and H. Wilczyński[1]

(1) H. Niewodniczański Institute of Nuclear Physics, ul. Radzikowskiego 152, 31-342 Kraków, Poland

(2) Forschungszentrum Karlsruhe, Institut für Kernphysik, 76021 Karlsruhe, Germany

Abstract

Using the CORSIKA shower simulation package, the spatial distribution of energy deposited by the shower in the atmosphere through ionization is obtained and the distribution of light arriving to the detector is calculated. The resulting shower image is compared with that obtained using the NKG distribution of particles in the shower and a constant fluorescence yield. Taking into account the distribution of energy deposited by the shower leads to a small dependence of the size of shower image on the primary particle.

1. Introduction

The fluorescence method of extensive air shower (EAS) detection is based on recording light emitted by air molecules, excited by charged particles of the shower. The amount of fluorescence light is closely correlated to the particle content of a shower and provides therefore a calorimetric measure of the primary energy. It has been commonly assumed that the fluorescence yield, i.e. the number of fluorescence photons emitted per unit length of a charged particle track, is approximately constant, the same for all particles in the shower. However, since the fluorescence light is induced by exciting the molecules of the ambient medium (the air), the fluorescence yield is expected to depend on the ionization density along a charged particle track [5]. Most particles in the shower have energies below 1 GeV, i.e. in the energy range of considerable dependence of ionization density on particle energy. Therefore, one should expect that the total fluorescence signal induced by the shower should depend not just on the number of particles in the shower, but rather on the total energy deposited in the air through ionization.

2. Simulations

In this paper we analyze the image of the shower using two different approaches. First: we keep the constant value of fluorescence yield $N_\gamma = 4.02$
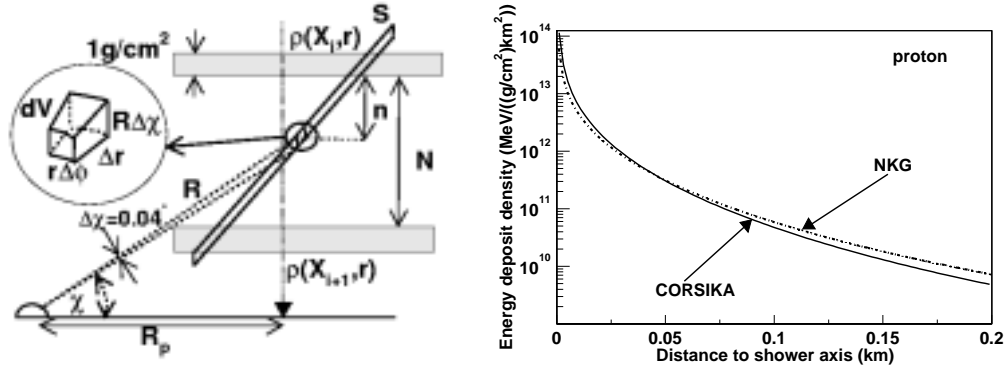
Fig. 1. (A-left) Geometry of an EAS as seen by the fluorescence detector. Photons which arrive simultaneously to the eye originate from surface S. (B-right) The lateral distribution of energy deposit density in CORSIKA and NKG approximations, calculated for an average vertical proton shower, with energy $E_0 = 10^{19}$ eV.

photons per meter, as used by the Fly's Eye group, and assume the NKG distribution of particles in the shower (NKG approximation). The lateral distribution of particles in the shower can be written as $\rho_N(X, r) = N(X)f(r)$, where $f(r)$ is the lateral shape function. The width of the shape function $f(r)$ is proportional to the width of the shower image. The size of the shower image $\Delta\theta$ is defined as the diameter of the shower image spot at an elevation angle χ, i.e. the apparent angular size of the surface S (see Fig.1), as seen from the detector. In the second approach using the CORSIKA shower simulation package [4,6], the lateral energy deposit distribution $\rho(X_i, r)$ is calculated at 20 horizontal layers of thickness $\Delta X = 1$ g/cm^2.

The photons which constitute an instantaneous image of the shower originate from a range of shower development stages, namely from surface S shown in Fig. 1. The small element of surface S in polar coordinates corresponds to a small volume ΔV. The value of energy deposit $\rho(X_n, r)$ in the volume ΔV at distance r can easily be constructed by linear interpolation, see Ref. [3] for more details. Using this interpolation, the number of photons N_γ from each volume element ΔV emitted towards the detector can be calculated.

In this way, the spatial distribution of points of origin of the simultaneous photons around the shower axis is obtained. These photons are propagated towards the fluorescence telescope, using the Hybrid_fadc simulation software [1]. The software incorporates the atmospheric light scattering mechanism: the Rayleigh scattering on molecules of air and Mie scattering on aerosols. The atmospheric attenuation is also accounted for, so that a total photon flux (including scattered Cherenkov photons) arriving at the detector is obtained. Finally, the angular distribution of these simultaneously arriving photons is constructed to form the image of the shower.
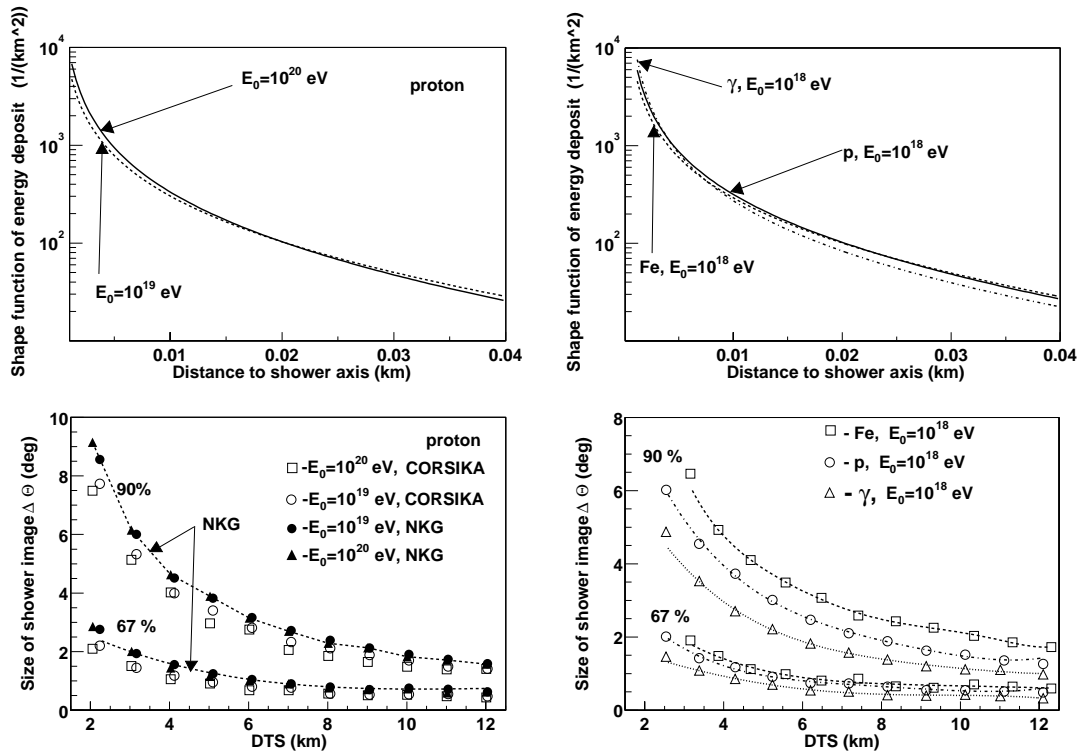
Fig. 2. (A-upper left) Shape function of average CORSIKA lateral distribution $f(r)$ vs distance to shower axis for vertical proton showers with different energies. (B-lower left) Size of the shower image containing 90% and 67% of light versus the detector to shower (DTS) distance, using CORSIKA and NKG distribution of energy deposit. (C-upper right) Shape function of average CORSIKA lateral distribution vs distance to shower axis r, for vertical proton, iron and γ shower. (D-lower right) Size of the shower image containing 90% and 67% of light versus detector to shower distance using CORSIKA distributions of energy deposit for iron, proton and γ primaries (at shower maximum).

3. Results and discussion

Simulation runs were done for primary proton, iron and γ showers with different energies of primary particle E_0. Vertical showers landing at variable core distance $R_p = 2, 3, ..., 11$ and 12 km were studied at their maxima.

Fig. 1B shows the calculated lateral distribution of the energy deposit versus distance to shower axis at any point of surface S. In case of the CORSIKA approach, the energy deposit density (solid line in Fig. 1B) was obtained using the two-dimensional histogram of energy deposited. It is seen that the energy deposit obtained using CORSIKA histograms becomes smaller than NKG for distances to shower axis greater than 45 m. This implies that locally one should expect

values of energy loss and also lateral distribution of particles in the shower which differ from those used in the NKG approximation. Since close to shower axis the value of energy deposit obtained by CORSIKA is greater than that from NKG, it means that there are more energetic particles close to the shower axis.

In Fig. 2A (upper left) the shape functions of CORSIKA lateral distributions for proton showers with primary energies $E_0 = 10^{20}$ and 10^{19} eV are shown. Fig. 2B (lower left) shows the size of the shower image $\Delta\theta$ containing 90% or 67% of light as a function of distance from the detector to the shower (DTS), for showers with different core distance R_p. It is seen that the spot size in the shower maximum is independent of energy in the NKG approximation and that the NKG approximation leads to larger sizes of shower image than those derived from CORSIKA. Moreover, for a shower with higher energy, the image size from CORSIKA is noticeably smaller than that from NKG. These differences can be understood taking into account differences of the shape function. Finally, we discuss the differences of the shower image between showers induced by different primary particles of the same energy. In Fig. 2C (upper right) the shape functions are presented for γ-, proton- and Fe-induced showers. One can see clear differences in the shape functions. The γ profile dominates over the other profiles at small distances ($r < 5$ m) from shower axis. On the other hand, Fe profile dominates at distances far from shower axis ($r > 23$ m). On the basis of Fig. 2C, one expects differences in the size of shower image. Thus, the image spot size of an Fe shower will be larger than the proton one, which in turn exceeds the spot size of a γ shower. This agrees with results presented in Fig. 2D (lower right). It can be seen that differences are quite considerable. We note that when just the *number of particles* is used (thus assuming implicitly the same ionization for all particles), there are no differences visible in the image spot size between proton and iron showers [2]. However, using the *distribution of deposited energy* leads to the difference in image size shown in Fig. 2D. Therefore, the study of shower image may be helpful in identification of primary particles.

1. Dawson B., private communication
2. Góra D. et al. 2001, Proc. 27th ICRC, Hamburg, **2** 543
3. Góra D. et al. 2002, Pierre Auger Project Note GAP-2003-057
4. Heck D. et al. 1998, Report FZKA 6019, Forschungszentrum Karlsruhe
5. Kakimoto F. et al. 1996, Nucl. Instr. Meth. **A 372** 527
6. Risse M. and Heck D. 2002, Pierre Auger Project Note GAP-2002-043